Paper No.
06365

CORROSION
NACExpo 2006
61ST ANNUAL CONFERENCE & EXPOSITION

BASICS REVISITED: KINETICS OF IRON CARBONATE SCALE PRECIPITATION IN CO_2 CORROSION

Wei Sun and Srdjan Nesic
Institute for Corrosion and Multiphase Technology
Ohio University
342 West State Street
Athens, Ohio 45701

ABSTRACT

Glass cell experiments were conducted to understand kinetics of iron carbonate scale formation in pure carbon dioxide (CO_2) corrosion of mild steel. Weight gain and loss (WGL) method was used as a direct approach to investigate kinetics of scale formation. The experiments were done at the temperatures of 60°C to 90°C, and an iron carbonate supersaturation range of 12 to 350. It is found that the calculated results obtained by the previous kinetics expressions using the traditional dissolved ferrous ion concentration method are one to two orders of magnitude higher than the experimental precipitation rates obtained in the present study by the WGL method. The results show that the main source of the ferrous ions which are involved in formation of the protective iron carbonate scale is the iron dissolution process. It has been clearly demonstrated that the precipitation rate of iron carbonate is directly related to the conditions at the steel surface which can frequently be very different from the one in the bulk fluid.

Keywords: kinetics, iron carbonate, scale, precipitation, CO_2 corrosion

INTRODUCTION

Surface scale formation is one of the important factors governing the rate of corrosion[1-3]. In the case of pure CO_2 corrosion, when the concentrations of Fe^{2+} and CO_3^{2-} ions exceed the solubility limit, solid iron carbonate precipitates[4, 5].

$$Fe^{2+} + CO_3^{2-} \Rightarrow FeCO_{3(s)} \quad (1)$$

The iron carbonate scale can slow down the corrosion process by presenting a diffusion barrier for the species involved in the corrosion process and by covering up a portion of the steel surface and preventing the underlying steel from further

dissolution. Iron carbonate scale growth depends primarily on the precipitation kinetics. Two different expressions (Equation 2 and 3) are used to describe the kinetics of iron carbonate precipitation in pure CO_2 corrosion (proposed respectively by Johnson and Tomson[6] in 1991 and van Hunnik et al.[7] in 1996). In both cases the rate of precipitation *PR* is a function of iron carbonate supersaturation *SS*, the solubility K_{sp}, temperature (via the kinetic constant k_r which obeys Arhenius law), and surface area-to-volume ratio *A/V*.

$$PR = k_r \frac{A}{V} K_{sp} \left\{ (SS)^{0.5} - 1 \right\}^2 \tag{2}$$

$$PR = k_r \frac{A}{V} K_{sp} (SS - 1)\left(1 - SS^{-1}\right) \tag{3}$$

Supersaturation *SS* is defined as species concentrations and the solubility limit:

$$SS = \frac{c_{Fe^{2+}} c_{CO_3^{2-}}}{K_{sp}} \tag{4}$$

The equation (2) given by Johnson and Tomson[6] was fitted with experimental results at the very low levels of supersaturation using a temperature ramp method. According to van Hunnik et al. [7] it overestimated the precipitation rate particularly at large supersaturations. The latter group proposed a nominally more accurate expression (3).

As a part of a larger project focusing on precipitation of iron carbonate and iron sulfide, expressions (2) and (3) were tested against independently generated precipitation kinetics data. It was found that for the case of iron carbonate precipitation both overestimated the magnitude of the precipitation rate by a large margin (factor 10-100). Therefore, it was concluded that a more thorough examination of the kinetics of iron carbonate scale precipitation in CO_2 corrosion needed to be done.

EXPERIMENTAL PROCEDURE

The present measurements were conducted in a glass cell as shown in Figure 1. The experiments were performed in stagnant solutions and 1 bar total pressure, the temperature varying from 60ºC to 90ºC. Initially each glass cell was filled with 2 liters of distilled water and 1% wt. NaCl. The solution was heated and purged with CO_2 gas. After the solution was deoxygenated, the pH was increased to the desired pH 6.6 by adding a deoxygenated sodium bicarbonate solution. Subsequently, the required amounts of Fe^{2+} were added in the form of a deoxygenated ferrous chloride salt ($FeCl_2.4H_2O$) solution. In various experiments supersaturation of iron carbonate in the solution was varied from 12 to 350 in order to investigate how supersaturation influenced the precipitation rate. Then rectangular specimens of X65 steel were inserted into the solution as substrates for growing the iron carbonate scale. Prior to immersion, the carbon steel specimen surfaces were polished with 240, 400 and 600

grit SiC paper, rinsed with alcohol and degreased using acetone. The chemical composition of the X65 steel used for all the experiments is shown in Table 1.

Both precipitation rate and corrosion rate were measured by weight gain/loss method[8] (WGL). Time-averaged precipitation rate of iron carbonate scale was obtained by subtracting the weight of the coupons which had iron carbonate scale and those after the scale was removed by using the Clarke solution. Time-averaged corrosion rate was calculated by subtracting the weight of the coupons prior to running the experiments and after removing the iron carbonate scale. A spectrophotometer was used to measure ferrous ion concentration in the solution. The coupon with the iron carbonate scale on it was observed using Scanning Electron Microscopy (SEM).

RESULTS

The experimental results obtained are presented below in the following manner:

- Verification experiments used to test/verify the existing precipitation rate expressions.
- Kinetics experiments used to investigate the effect of temperature and supersaturation on precipitation rate.

Verification experiments

Three sets of experiments were conducted in order to verify the precipitation rate expressions, using X65 carbon steel substrates with different surface areas at pH 6.6, temperature of 80^{o}C, initial Fe^{2+} 50ppm (which then drifted down as precipitation occurred), The first set of experiments was conducted using one specimen with the surface area of 5.4 cm^2. The second set of experiments was conducted using thirty specimens each having a surface area of 2 cm^2 (total of 60 cm^2). During these experiments, six specimens were taken out of the solution every two and a half hours. In the third set of experiments twelve specimens each having a surface area of 21cm^2 (total of 252 cm^2) were inserted in the solution and three specimens were taken out every two and a half hours.

It should be noted that both Johnson and Tomson[6] and van Hunnik et al. [7] determined experimentally the precipitation rate of iron carbonate by an indirect technique which is based on measuring the decrease of ferrous ion concentration in the bulk of the solution (referred to as the "Fe^{2+} method" in the text below). It was implicitly assumed that the entire amount of ferrous ion "lost" by the solution ends up as precipitated iron carbonate scale on the steel surface. In the present experiments, the same was done, ferrous ion concentrations was measured at different times. The results show that the change of ferrous ion concentration in the solution with time was similar irrespective of the very different surface areas of the substrates (see Figure 2) i.e. using this method very similar precipitation rates were obtained for all surface area-to-volume ratios tested. However, according to the Johnson and Tomson[6] and van Hunnik et al. [7] i.e. expressions (2) and (3), this should not happen, rather the precipitation rate should be directly proportional to the surface area-to-volume ratio

A/V. Therefore, either the expressions (2) and (3) or the experimental technique had to be wrong.

When the precipitation rates calculated by the Fe^{2+} method were compared to those obtained by the more direct weight gain/loss (WGL) method it became clear where the problem lies. The results shown in Figure 3 illustrate that the precipitation rate does indeed depend on the *A/V* ratio as expected and that the Fe^{2+} method can be in gross error. When using substrates with a large surface area of 252cm^2 (large *A/V*), similar precipitation rate are obtained by using both the WGL and the Fe^{2+} methods. However, with the decrease of the surface area of the substrate, the precipitation rate measured by the weight gain/loss method decreases while the one measured by the Fe^{2+} method does not, as previously noted. A simple mass balance for Fe^{2+} has shown that in the experiments with the small substrates (small *A/V*) most of the precipitated iron carbonate does not end up on the steel surface and therefore the key assumption implicit for this method fails. For large *A/V*, most of the iron carbonate precipitates on the steel substrate and the assumption holds hence the Fe^{2+} method appears to be valid. On the other hand, the WGL method, while being more tedious, offers a more realistic estimate of the precipitation rate under all conditions. Results obtained for various *A/V* ratios all fall within the expected error margins as shown by the error bars in Figure 3. From the same figure it should be noted that the discrepancy between the two methods is smaller for smaller supersaturations.

It was impossible to reproduce directly the original experiments of Johnson and Tomson[6] and van Hunnik et al. [7] since not sufficient detail is reported in the original publications. However predictions made by the expressions (2) and (3), which were derived from their original data, were compared to the present measurements of the precipitation rate and, not surprisingly, large discrepancies were found. For example, Figure 4 shows that the more accurate WGL experimental data are up to two orders of magnitude lower when compared to the calculated results using the more recent van Hunnik et al. [7] expression (3). However, the agreement "improves" when one compares the same predictions with the precipitation data obtained by the Fe^{2+} method for small *A/V* ratios, which we now know are erroneous. Therefore it is concluded that both expressions (2) and (3) overestimate the actual precipitation rate by a large margin because the experimental data used to derive them were based on the Fe^{2+} method which is unreliable.

Kinetics experiments

Kinetics precipitation kinetics experiments were conducted in a stagnant solution. In the first series of experiments initial Fe^{2+} of 50 ppm decreased as precipitation proceeded, pH 6.6 and a range of temperatures was used varying from 60^{o}C to 90^{o}C. The exposed area of each coupon is approximately 21cm^2 which is large enough to measure the weight of iron carbonate film accurately. Figure 5 shows the change of ferrous ion concentration in the solution at different temperatures. The ferrous ion concentration in the solution at 60^{o}C increased initially because of the corrosion of carbon steel which overpowered the precipitation process, and then decreased gradually with temperature as the corrosion rate decreased. When the temperature increased to 70^{o}C, 80^{o}C and 90^{o}C, the ferrous ion concentration decreased

steadily. Based on the rate of change of ferrous ion concentration it can be seen that the precipitation rate increased with the increase of temperature.

The precipitation rate obtained by the WGL method as a function of time and supersaturation of iron carbonate at temperatures of 60°C is illustrated in Figure 6. The error bars represent the maximum and minimum measured precipitation rates. The precipitation rate at the temperature of 60°C increased with the increase of precipitation time during the first five hours and then became stable between 5 hours and 7.5 hours. From 7.5 hours to 10 hours the precipitation rate decreased because of the decrease of supersaturation in the bulk of the solution. The corrosion rate of carbon steel under the test conditions is below 1mm/year (Figure 7). Comparing the precipitation rate with the corrosion rate in the same units (mol/h/m^2), it is found that the precipitation rate is slightly higher than the corrosion rate in the first 5 hours. After 5 hours, the precipitation rate is slightly lower than the corrosion rate. The source of Fe^{2+} forming iron carbonate scale includes both Fe^{2+} released from the steel surface and Fe^{2+} provided by the bulk of the solution. Hence it is important to understand the conditions on the steel surface because the corrosion rate has a significant effect on the precipitation rate of iron carbonate scale.

Similar trend in the experimental results was obtained in the experiments at the temperature of 70°C. The precipitation rate of iron carbonate and the corrosion rate of carbon steel are shown in Figure 8 and Figure 9. The precipitation rate increased with the increase of reaction time and then decreased after 7.5 hours.

At 80°C, the precipitation rate decreased steadily with time because of the decrease of the super saturation in the bulk of the solution (Figure 10). The corrosion rates obtained by the WGL method are shown in Figure 11. Since iron carbonate films formed faster at higher temperature and were more protective, the corrosion rate decreased more with the increase of temperature. Comparing the precipitation rate with the corrosion rate in the same units, the precipitation rate is higher than the corrosion rate at any time in the experiments, which proves that the bulk Fe^{2+} is a more significant source of ferrous ions forming iron carbonate scale at 80°C than at the lower temperatures. Similar experimental results were obtained at 90°C (Figure 12 to Figure 13).

The scaling tendency:

$$ST = \frac{PR}{CR} \tag{5}$$

where *PR* is the precipitation rate of iron carbonate, *CR* is the corrosion rate of the steel. The scaling tendency was calculated by using the same molar units (mol/h/m^2) for precipitation rate and the corrosion rate and is shown in Figure 14 for various experiments. The scaling tendency at the temperature of 60°C and 70°C varies from 0.5 to 1.5. With the temperature increasing to 80°C and 90°C, the scaling tendency increases above 1.5, suggesting more rapid scaling and more effective protectiveness at higher temperature.

The morphology and cross section of iron carbonate scale at different temperature (70°C and 80°C) as a function of time are shown in Figure 15 and Figure 16. Clearly the iron carbonate films became denser and therefore more protective over time. By comparing the appearance of iron carbonate film shown in Figure 17 for various temperatures, it can be seen that the surface coverage by iron carbonate scale increased with the increase of temperature. The calculated porosity of the iron carbonate scale under the different test conditions is between 0.6 and 0.85, as shown in Table 2.

A series of more complicated experiments was conducted at constant supersaturation in stagnant solution under the condition at Fe^{2+} 50ppm and 10ppm, pH 6.6 and temperature of 80°C. The constant supersaturation was achieved by continuously dosing a ferrous chloride solution to the glass cell to compensate for the Fe^{2+} ions lost by precipitation. Figure 18 illustrates that the precipitation rate for Fe^{2+}=50ppm was stable over time while the supersaturation was kept approximately 200. The corrosion rate was below 0.2mm/year (Figure 19) after three and a half hours. Figure 20 shows the precipitation rate vs. time at Fe^{2+}=10ppm and supersaturation of 100. The results show that the precipitation rate in the first 12 hours is slightly lower than the precipitation rate in the second 12 hours. The final corrosion rate decreased to very low values (Figure 21), which proved that protective iron carbonate scale formed on the steel surface after 36 hours. Overall, this series of experiments was consistent with the previous series where supersaturation changed in the course of the experiment, and has proven that by controlling the key parameters stable and reproducible results for iron carbonate precipitation kinetics can be obtained.

CONCLUSIONS

- The weight gain/loss method is a more reliable method for obtaining the precipitation rate when compared to the previously used techniques involving ferrous ion concentration method. The calculated results obtained by previous kinetics expressions using the traditional dissolved ferrous ion concentration method overestimate the precipitation rate by a large margin.
- The source of ferrous ions forming iron carbonate scale includes ferrous ions both released from the steel surface and those provided by the bulk of the solution. The precipitation rate of iron carbonate is directly related to corrosion and the conditions at the steel surface.
- The precipitation rate of iron carbonate scale is more strongly affected by the corrosion rate of the steel at low supersaturation. At high supersaturation, the corrosion rate has little effect on the precipitation rate.
- As expected the precipitation rate is a function of supersaturation and temperature.

ACKNOWLEDGEMENT

The authors would like to acknowledge the companies who provided the financial support and technical guidance for this project. They are BP, Champion Technologies, Clariant, ConocoPhillips, ENI, ExxonMobil, MI Technologies, Nalco, Saudi Aramco, Shell, and Total.

REFERENCES

1. A. K. Dunlop, H. L. Hassell and P.R. Rhodes, "Fundamental considerations in sweet gas well corrosion", Advances in CO_2 Corrosion, Ed. R. H. Hausler and H.P. Godard., Houston, Texas, National Association of Corrosion Engineers, 1984.

2. A. Ikeda, M. Ueda, and S. Mukai, "CO_2 behavior of carbon and Cr steels", Advances in CO_2 Corrosion, Ed. R. H. Hausler and H. P. Godard., Houston, Texas, National Association of Corrosion Engineers, 1984.

3. K. Videm, and A. Dugstad, "Corrosion of carbon steel in an aqueous carbon dioxide environment", Material Performance, 1989, March, 63-67.

4. A. Dugstad, "Formation of protective corrosion flims during CO_2 corrosion of carbon steel", Eurocorr 1997, Conf. of European Federation of Corrosion, held Sept. 22-25 (London, U.K.: Institute of Materials, 1997).

5. A. Dugstad, "Mechanism of protective film formation during CO_2 corrosion of carbon steel", Corrosion/98, Paper no. 31, NACE International, Houston, Texas, 1998.

6. M. L. Johnson and M. B. Tomson, "Ferrous carbonate precipitation kinetics and its impact CO_2 corrosion," Corrosion/91, Paper no. 268, NACE International, Houston, Texas, 1991.

7. E. W. J. van Hunnik and E. L. J. A. Hendriksen, "The formation of protective $FeCO_3$ corrosion product layers," Corrosion/96, Paper no. 6, NACE International, Houston, Texas, 1996.

8. K. Chokshi, W. Sun, and S. Nesic, "Iron carbonate scale growth and the effect of inhibition in CO_2 corrosion of mild steel" Corrosion/2005, Paper no. 05285, NACE International, Houston, Texas, 2005.

TABLES

Table 1. Chemical Composition of X65 (wt.%) (Fe is the balance)

Al	As	B	C	Ca	Co	Cr	Cu	Mn	Mo	Nb
0.0032	0.005	0.0003	0.050	0.004	0.006	0.042	0.019	1.32	0.031	0.046
Ni	P	Pb	S	Sb	Si	Sn	Ta	Ti	V	Zr
0.039	0.013	0.020	0.002	0.011	0.31	0.001	0.007	0.002	0.055	0.003

Table 2. The thickness and porosity of films at different reaction times for initial Fe^{2+} concentration of 50ppm, stagnant conditions and pH 6.6, T=80^{o}C.

T (^{o}C)	Reaction time (hrs)	Thickness of films (um)	Porosity
60	2.5	1	0.71
	5	2	0.59
70	2.5	2	0.81
	5	4	0.73
	7.5	8	0.78
	10	10	0.78
80	2.5	4	0.79
	5	6	0.79
	7.5	8	0.84
	10	8	0.82
90	2.5	4	0.79
	5	6	0.76

FIGURES

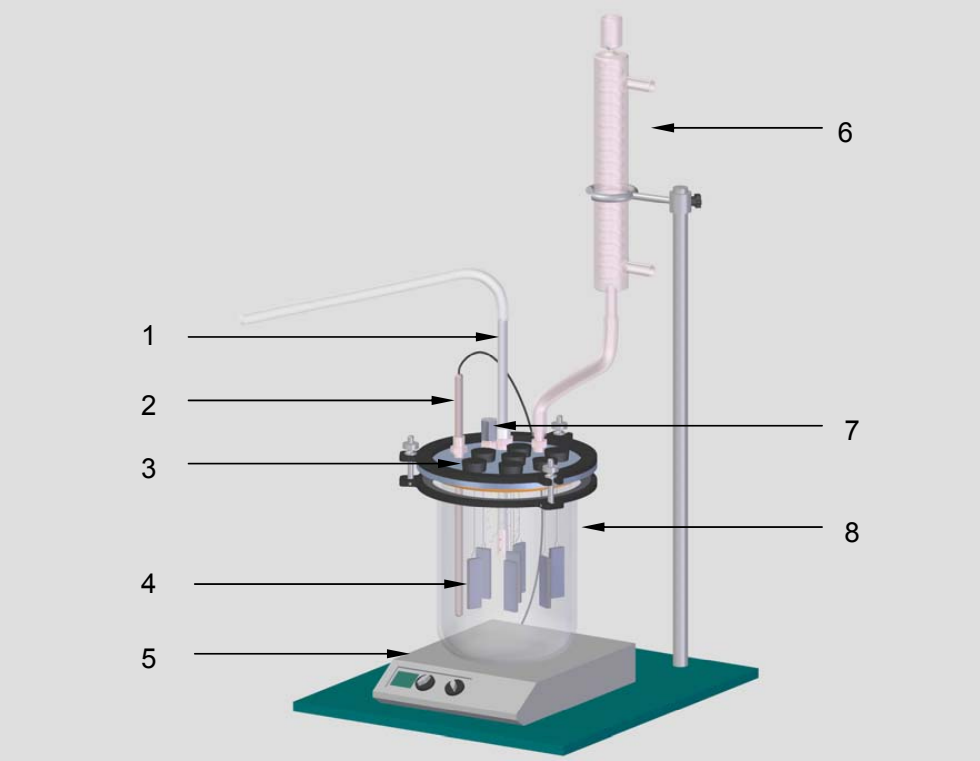

Figure 1. Schematic of the experimental test cell: 1. bubbler; 2. temperature probe; 3. rubber cork with nylon cord; 4. steel substrate; 5. hot plate; 6. condenser; 7. pH probe; 8. glass cell.

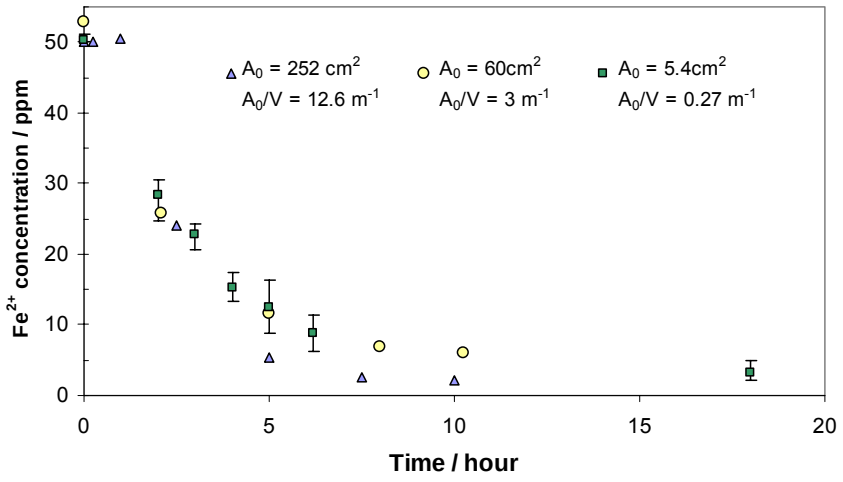

Figure 2. Ferrous ion concentration vs. reaction time for different surface areas of X65 steel substrates in pure CO_2 corrosion at pH 6.6, T=80°C stagnant conditions.

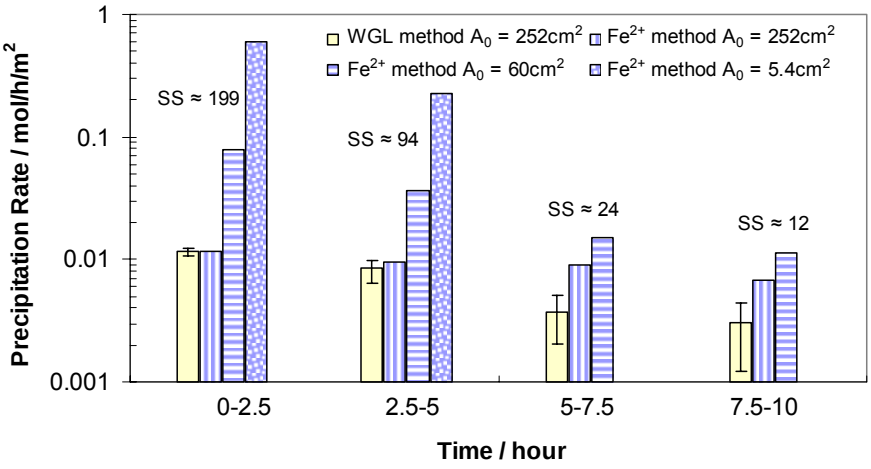

Figure 3. The comparison of differential precipitation rate of iron carbonate films on X65 carbon steel in different techniques (weight gain/loss method and Fe^{2+} concentration measurement) and for different surface areas of substrates (initially A_0 = 252cm^2, 60cm^2, and 5.4cm^2, which mean A_0/V = 12.6m^{-1}, 3m^{-1}, and 0.27m^{-1}) in pure CO_2 corrosion under the conditions of initial Fe^{2+} concentration 50ppm (which then drifted down), pH 6.6, T=80°C.

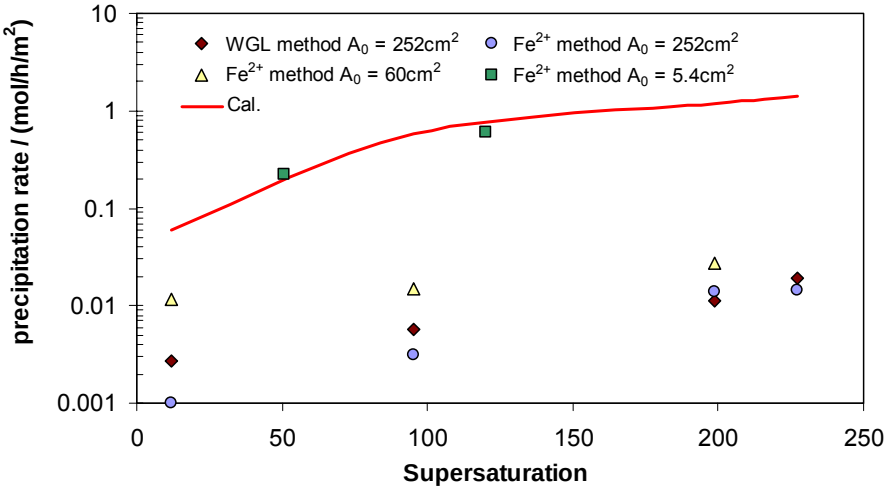

Figure 4. Experimental and calculated (using kinetics expression given by **v**an Hunnik et al. [7]) precipitation rates of iron carbonate under supersaturations of 12 to 250 at a temperature of 80°C.

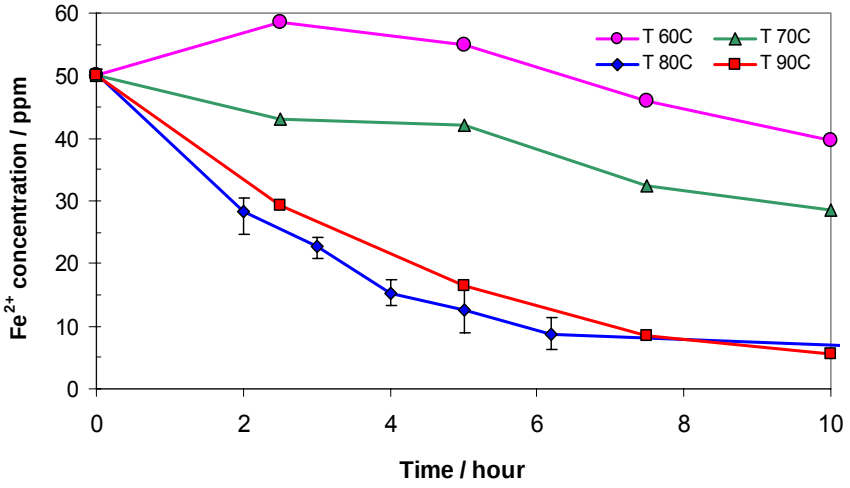

Figure 5. Fe^{2+} concentration vs. the reaction time in pure CO_2 corrosion under the conditions of initial Fe^{2+} concentration 50ppm (which then drifted down), pH 6.6, T of 60°C, 70°C, 80°C, 90°C.

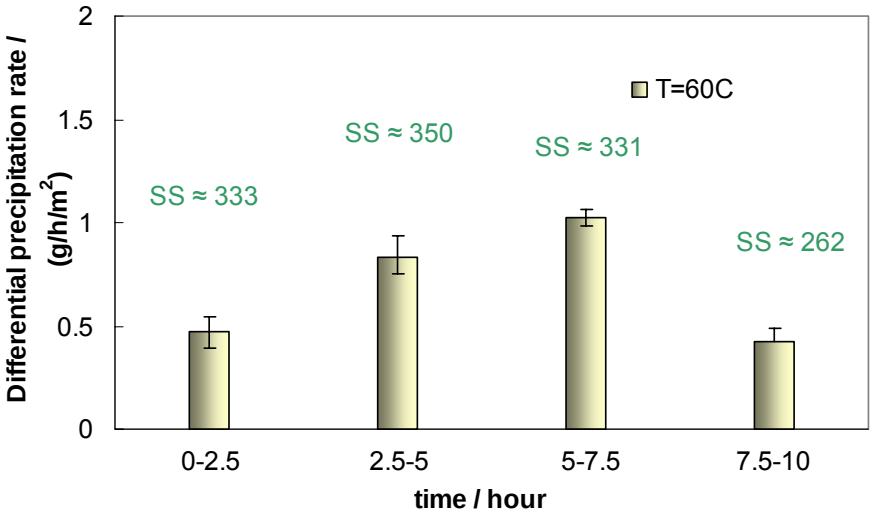

Figure 6. Differential precipitation rate of iron carbonate films on X65 carbon steel in pure CO_2 corrosion under the conditions of initial Fe^{2+} concentration 50ppm (which then drifted down), pH 6.6, T 60°C.

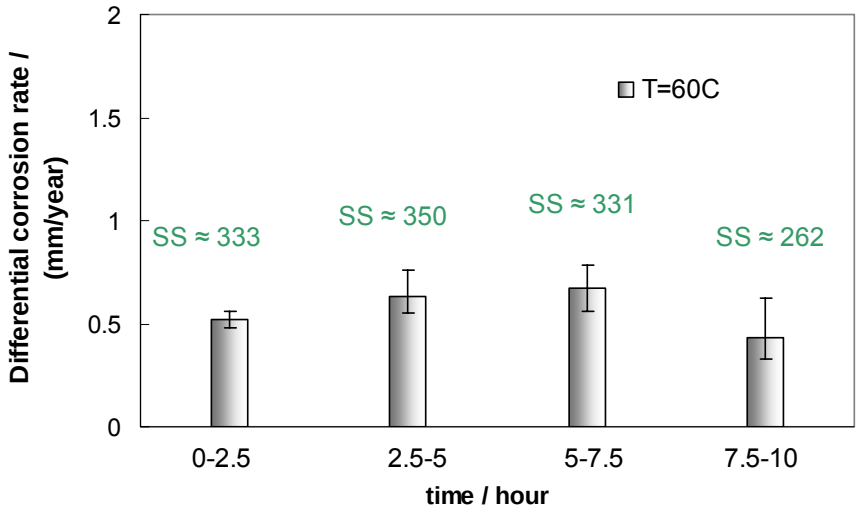

Figure 7. Corrosion rate of X65 carbon steel in pure CO_2 corrosion under the conditions of initial Fe^{2+} concentration 50ppm (which then drifted down), pH 6.6, T 60°C.

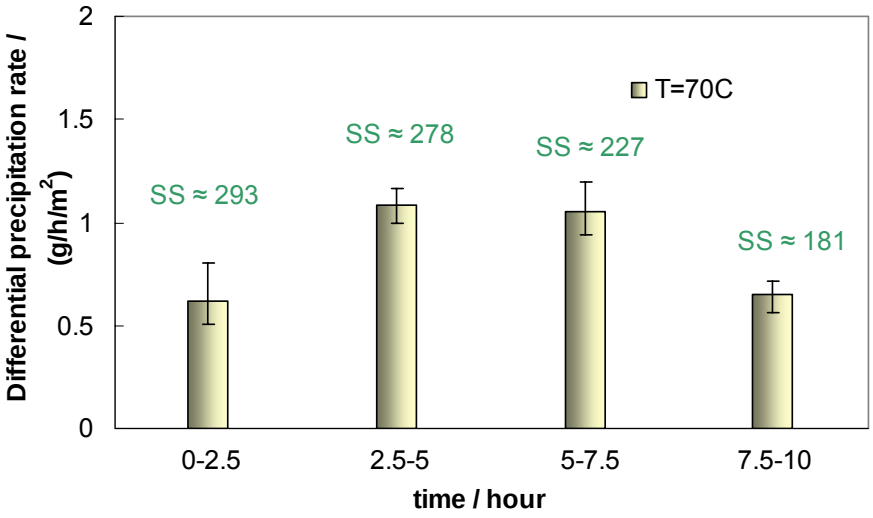

Figure 8. Differential precipitation rate of iron carbonate films on X65 carbon steel in pure CO_2 corrosion under the conditions of initial Fe^{2+} concentration 50ppm (which then drifted down), pH 6.6, T 70°C.

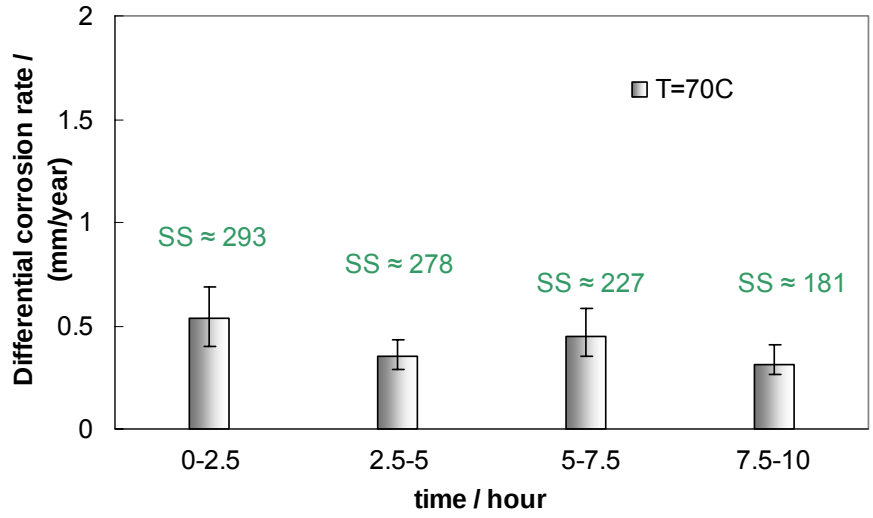

Figure 9. Corrosion rate of X65 carbon steel in pure CO_2 corrosion under the conditions of initial Fe^{2+} concentration 50ppm (which then drifted down), pH 6.6, T 70°C.

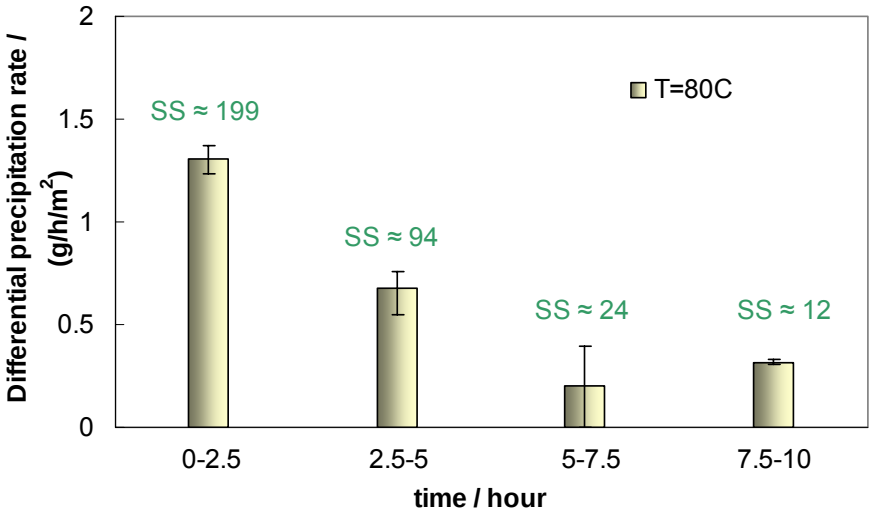

Figure 10. Differential precipitation rate of iron carbonate films on X65 carbon steel in pure CO_2 corrosion under the conditions of initial Fe^{2+} concentration 50ppm (which then drifted down), pH 6.6, T 80°C.

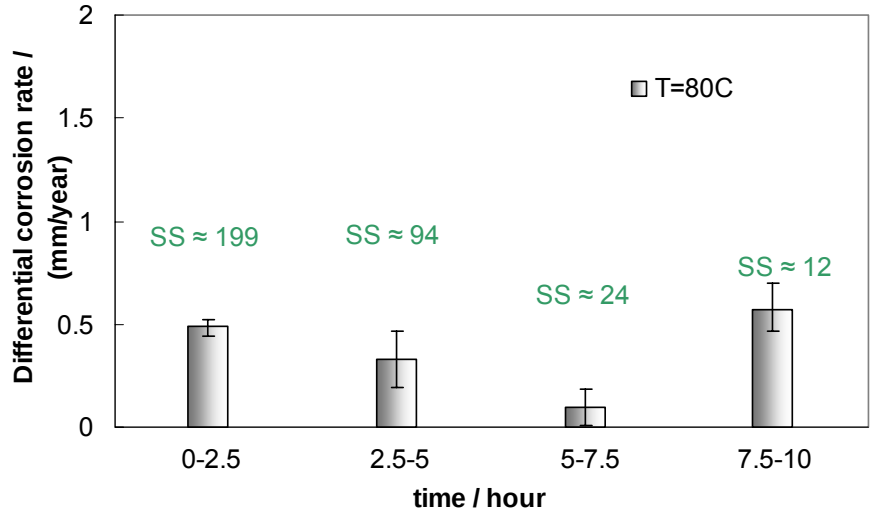

Figure 11. Corrosion rate of X65 carbon steel in pure CO_2 corrosion under the conditions of initial Fe^{2+} concentration 50ppm (which then drifted down), pH 6.6, T 80°C.

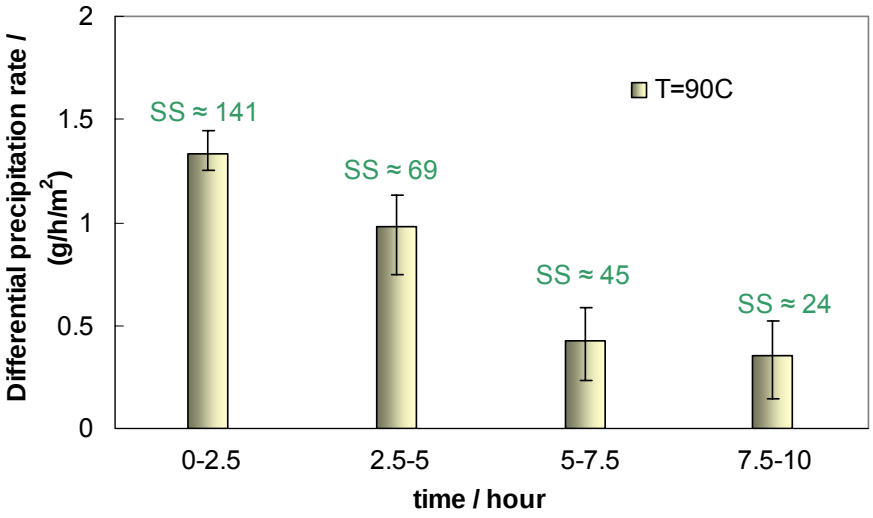

Figure 12. Differential precipitation rate of iron carbonate films on X65 carbon steel in pure CO_2 corrosion under the conditions of initial Fe^{2+} concentration 50ppm (which then drifted down), pH 6.6, T 90°C.

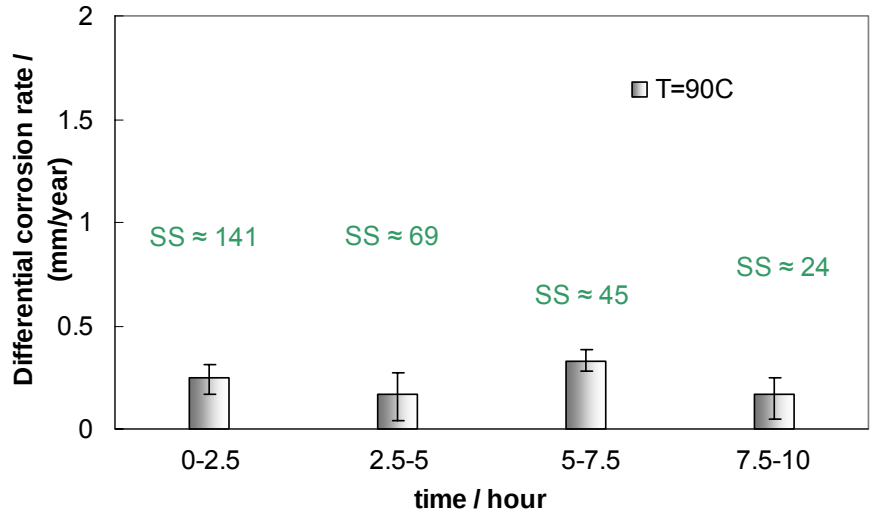

Figure 13. Corrosion rate of X65 carbon steel in pure CO_2 corrosion under the conditions of initial Fe^{2+} concentration 50ppm (which then drifted down), pH 6.6, T 90°C.

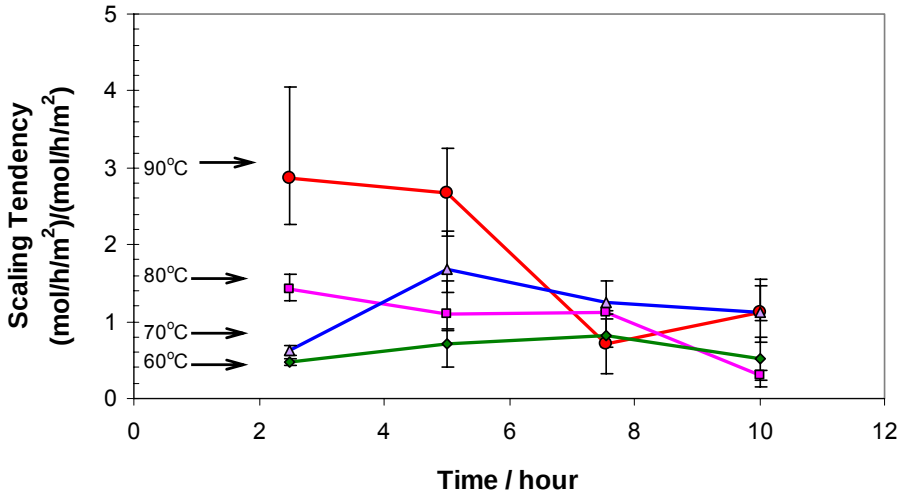

Figure 14. The comparison of scaling tendency in pure CO_2 corrosion under the conditions of initial Fe^{2+} concentration 50ppm (which then drifted down), pH 6.6, T 60°C, 70°C, 80°C, and 90°C.

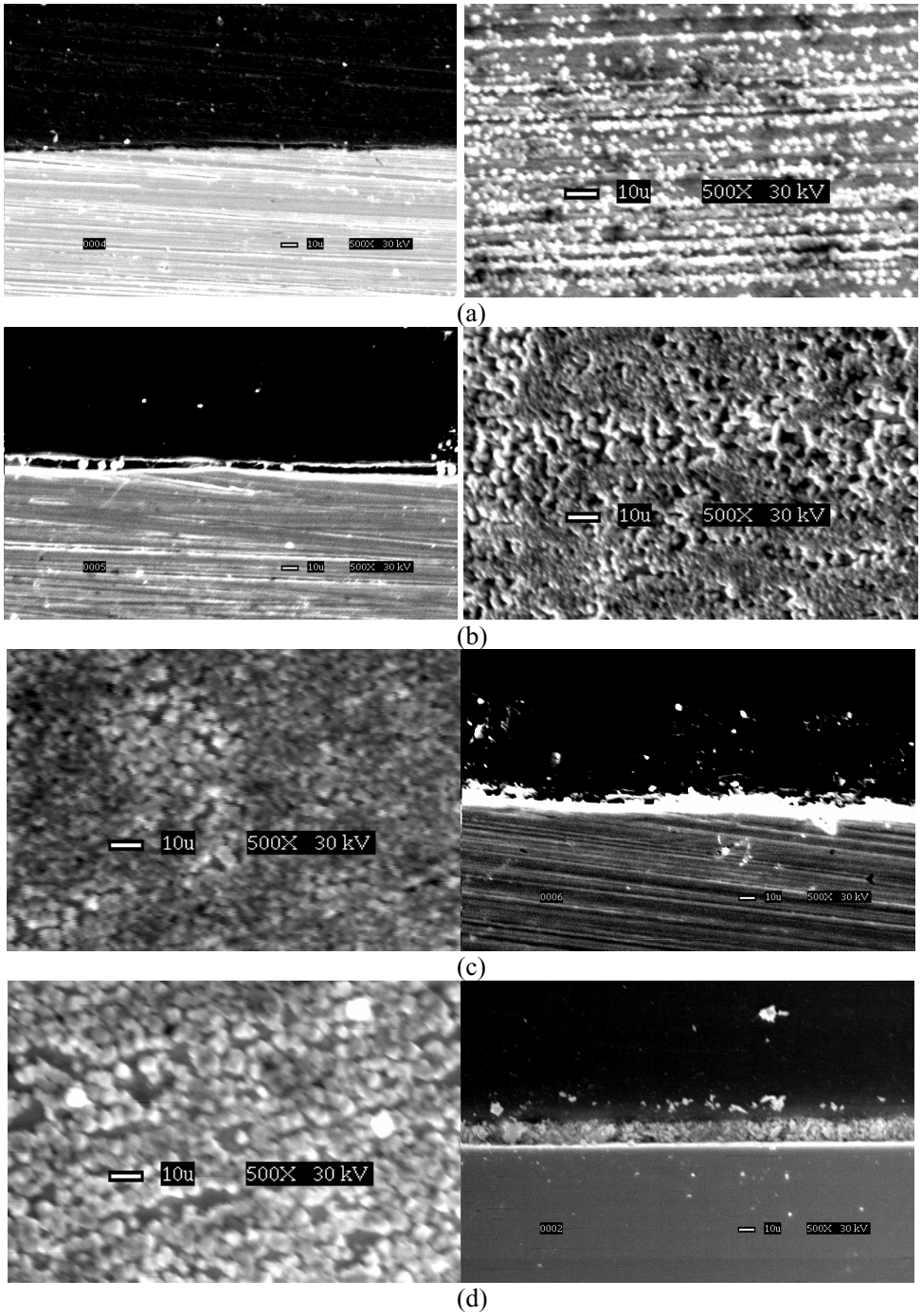

Figure 15. The morphology and cross section of iron carbonate after a) 2.5, b) 5, c) 7.5 and d) 10 hours (pH 6.6, T 70^{o}C, initial Fe^{2+} =50ppm (which then drifted down))

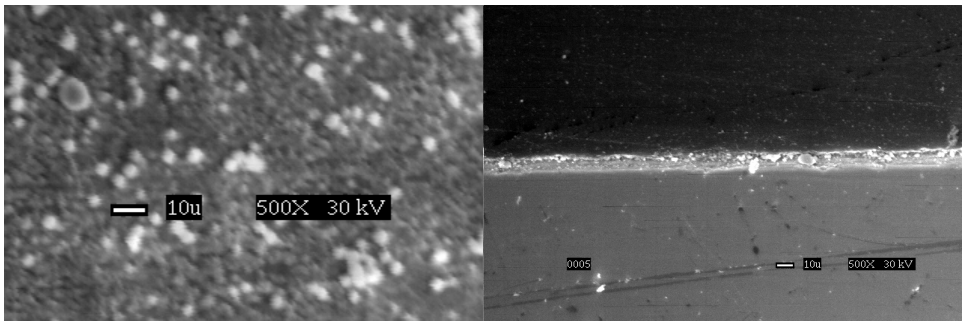

(a)

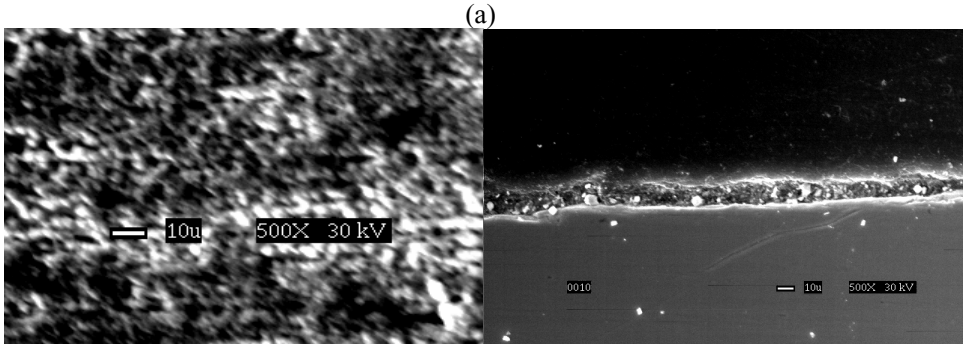

(b)

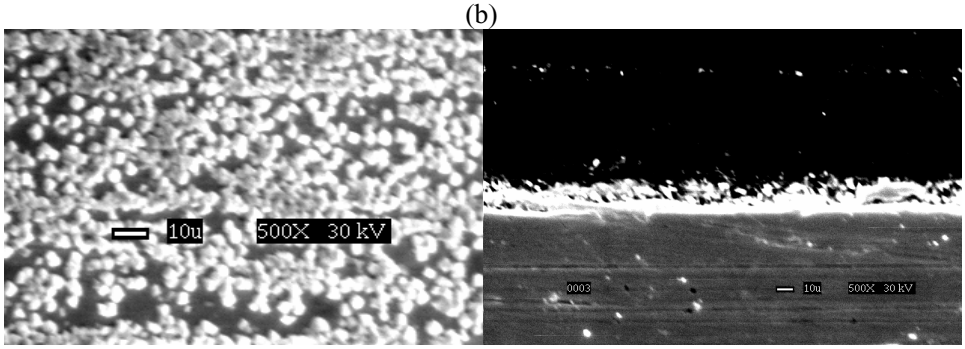

(c)

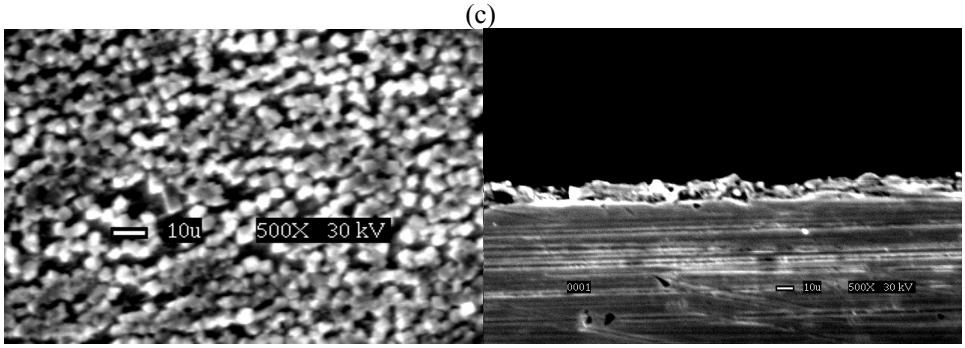

(d)

Figure 16. The morphology and cross section of iron carbonate after a) 2.5, b) 5, c) 7.5 and d) 10 hours (pH 6.6, T 80^{o}C, initial Fe^{2+} =50ppm (which then drifted down))

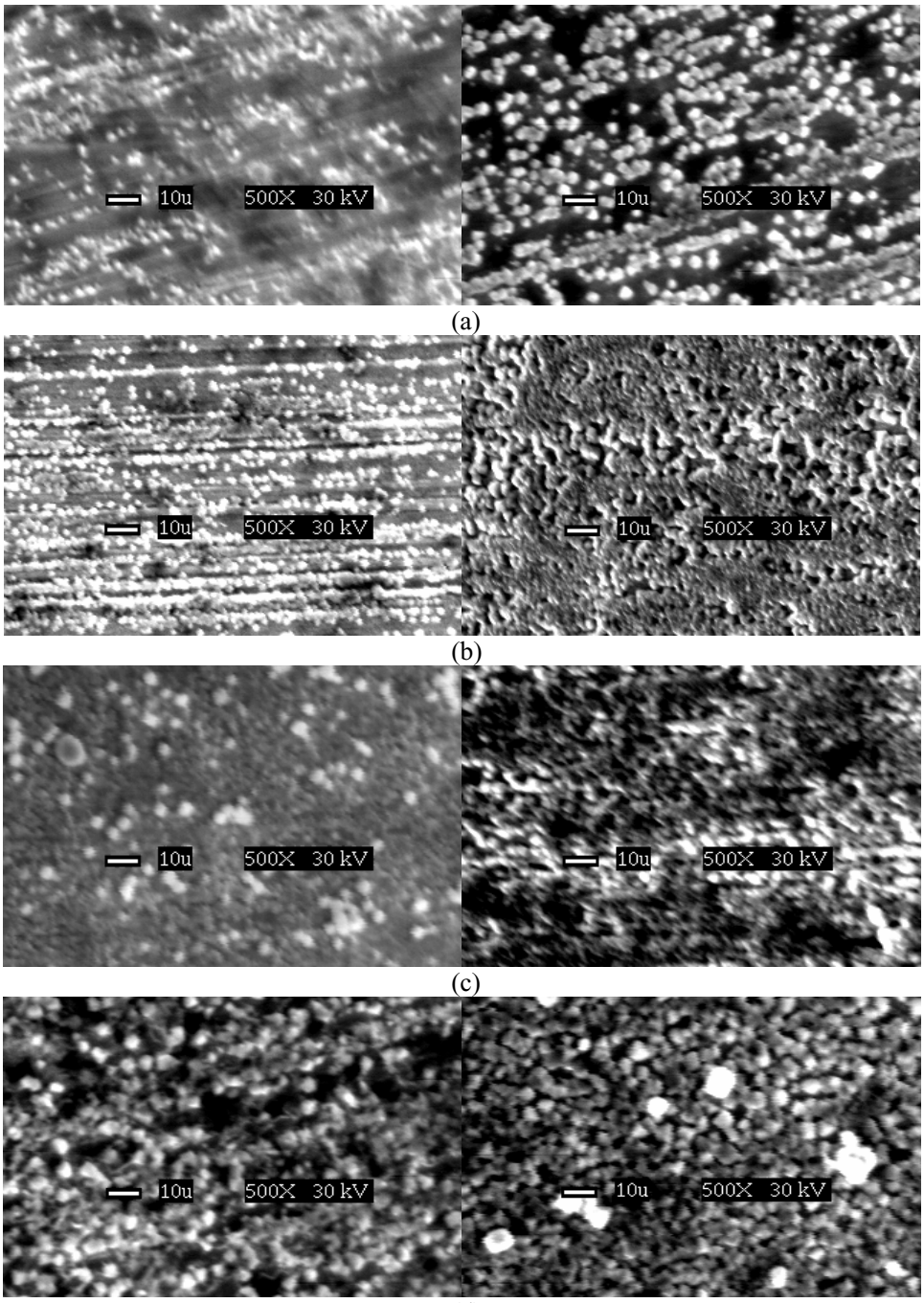

Figure 17. The morphology of iron carbonate in 2.5 and 5 hours at the temperatures of a) 60°C, b)70°C , c) 80°C and d) 90°C (pH 6.6, initial Fe^{2+} =50ppm (which then drifted down)) .

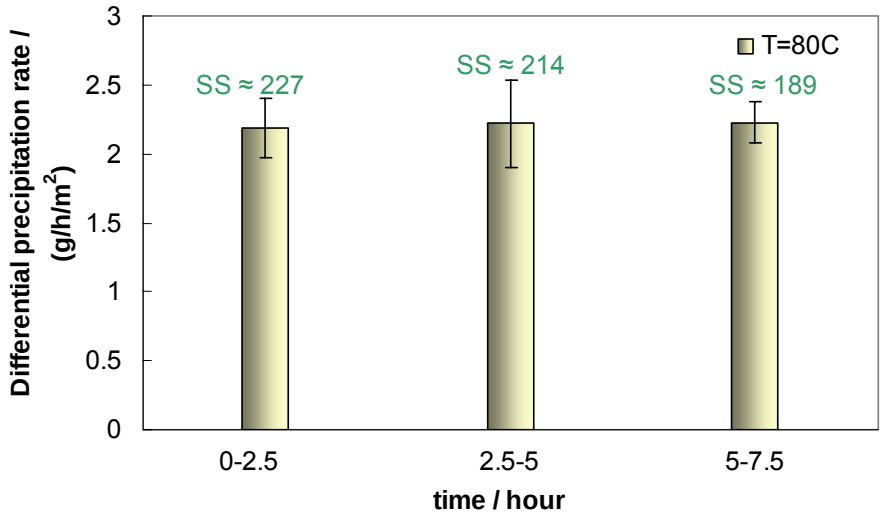

Figure 18. Differential precipitation rate of iron carbonate films on X65 carbon steel in pure CO_2 corrosion for constant Fe^{2+} concentration 50ppm, pH 6.6, T 80°C.

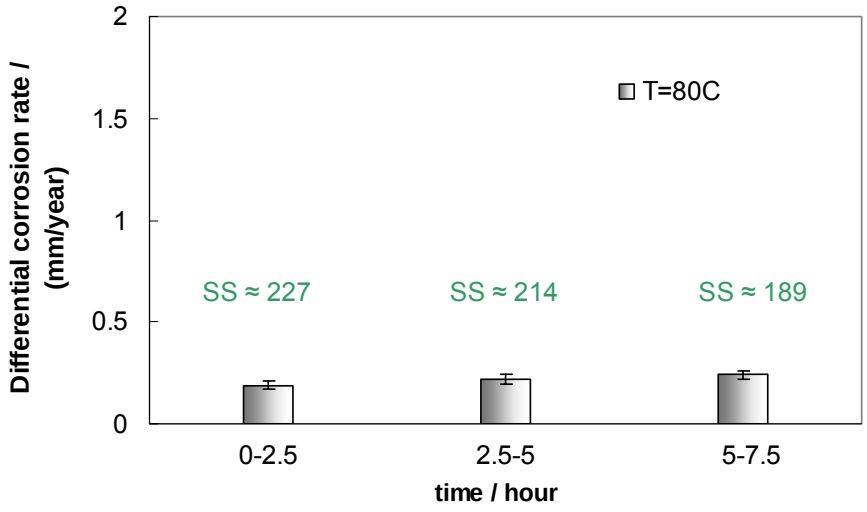

Figure 19. Corrosion rate of X65 carbon steel in pure CO_2 corrosion for constant Fe^{2+} concentration 50ppm, pH 6.6, T 80°C.

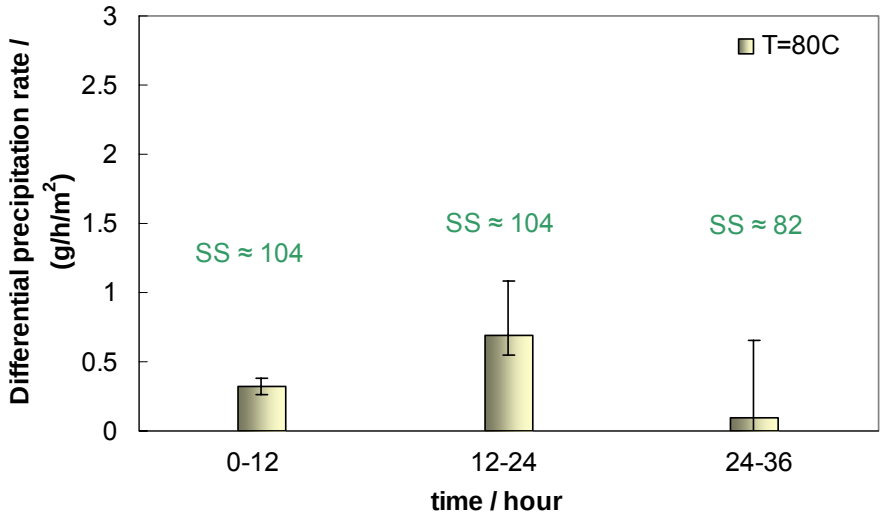

Figure 20. Differential precipitation rate of iron carbonate films on X65 carbon steel in pure CO_2 corrosion for constant Fe^{2+} concentration 10ppm, pH 6.6, T 80°C.

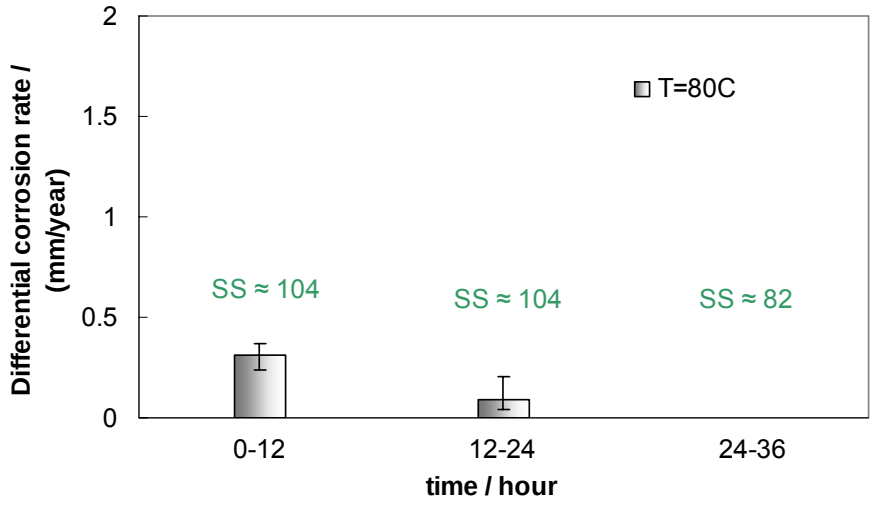

Figure 21. Corrosion rate of X65 carbon steel in pure CO_2 corrosion for constant Fe^{2+} concentration 10ppm, pH 6.6, T 80°C.